Folic Acid/Methotrexate Functionalized Mesoporous Silica Nanoflakes from Different Supports: Comparative Study

Martyna Trukawka, Krzysztof Cendrowski, Wojciech Konicki and Ewa Mijowska

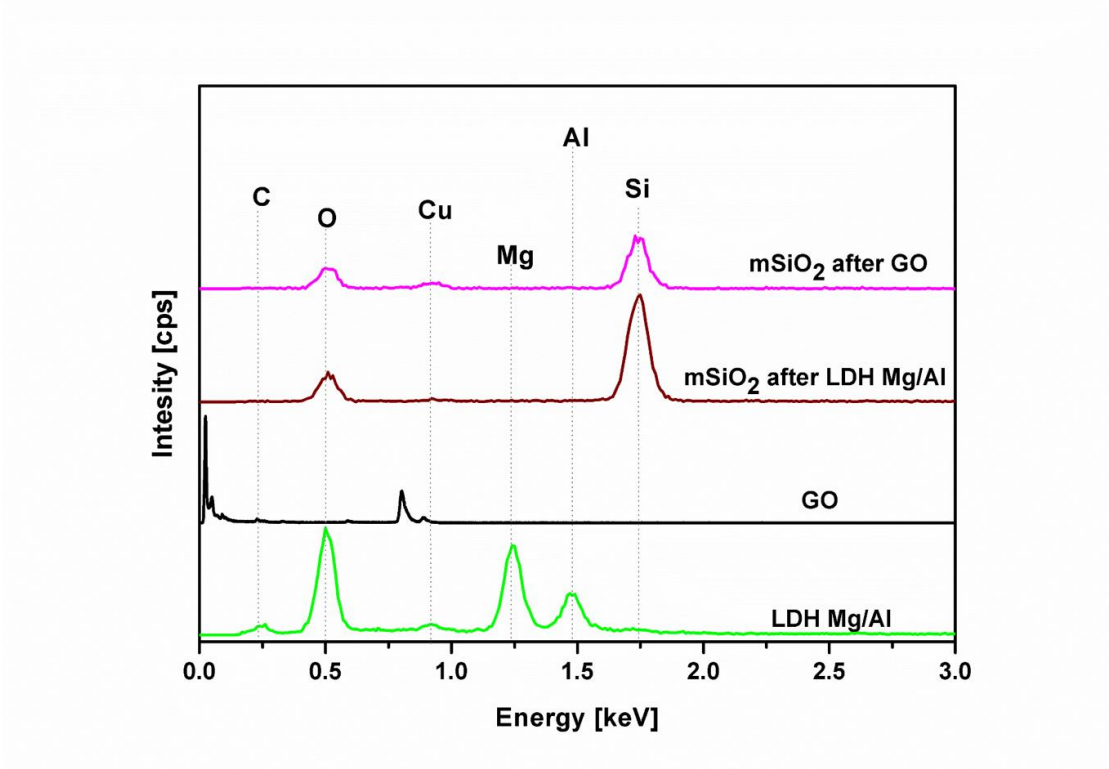

Figure S1. X-ray dispersion spectroscopy (EDX) elemental spectra of silica flakes and the templates.

Figure S2 presents XRD patterns of GO, $mSiO_2$ after GO, LDH Mg/Al, and $mSiO_2$ after LDH Mg/Al. The GO pattern exhibits a strong peak at $2\theta=11.28°$ corresponding to the (002) plane of GO, which confirms the successful preparation of GO from graphite powder through oxidation by the modified Hummers method [1]. The LDH Mg/Al pattern exhibits a series of reflections at 11.65°, 23.32°, 34.89°, 39.44°, 46.75°, 60.73°, and 62.10°. Sharp, intense peaks at low diffraction angles (peaks close to 11.71°, 23.53°, and 34.73°) were ascribed to diffraction by basal planes (003), (006), and (009), respectively [2]. The pattern of the $mSiO_2$ shows the broad peak at 22°, indicating that the flakes are composed of amorphous silica [3]. The lack of other diffraction peaks indicates the efficient removal of the templates from the silica flakes.

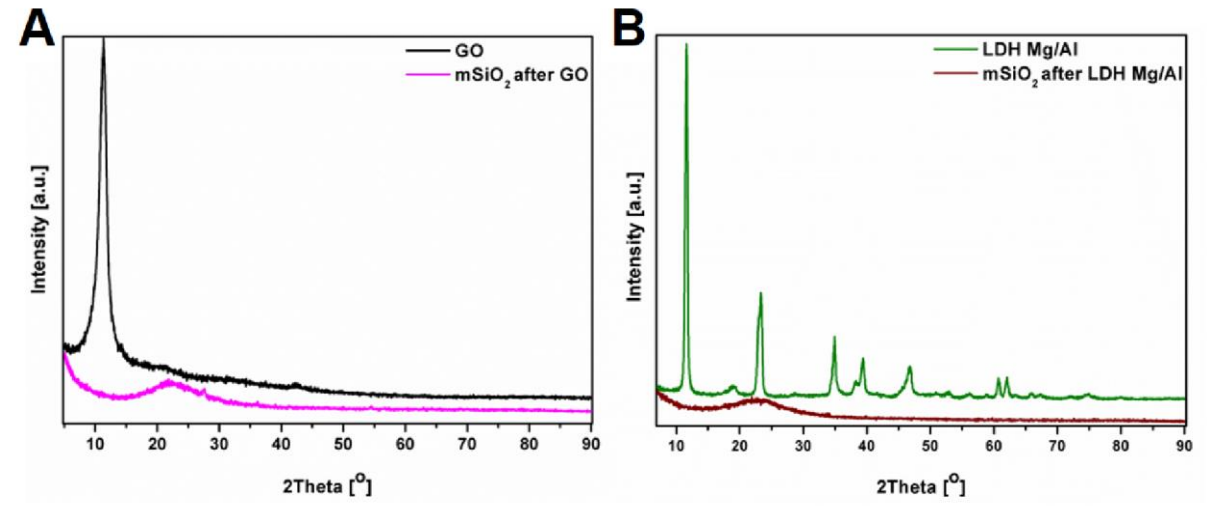

Figure S2. XRD patters of $mSiO_2$ after GO (**A**) and GO and $mSiO_2$ after LDH Mg/Al and LDH Mg/Al (**B**).

In Raman spectrum of graphene oxide (Figure S3A), two typical modes are observed: a D-band at 1332 cm^{-1} and a G-band at 1612 cm^{-1}. The G-band is characteristic for graphitic sheets, corresponding to a well-defined sp^2 carbon-type structure, whereas the D-band can be attributed to the presence of defects within the graphitic structure [4]. In the case of silica flakes, their Raman spectra are dominated by two spectral regions. The band in the range of 440–530 cm^{-1} involves motions of O in Si–O–Si symmetric stretching–bending modes. The peaks above 600 cm^{-1} are correlated to the Si–O stretching mode [5]. In the spectra of silica flakes, there are no peaks that are characteristic for them. This indicates the efficient removal of the matrix. The Raman spectrum of LDH Mg/Al exhibits several strong bands (Figure S3 B). The band at 548 cm^{-1} is from the stretching vibrations of Al–O–Mg bands, whereas the band around 483 cm^{-1} was assigned to hydroxyl groups [6]. The strongest peak at 155 cm^{-1} is possibly due to the hydrogen bonding and asymmetric stretching vibrations in LDH Mg/Al layers and interlayer water molecules [7,8]. The signal at 1052 cm^{-1} was identified as the Al–O bending mode [9]. Raman peaks around 1315 cm^{-1} are associated to the characteristics peaks of Mg–O [10].

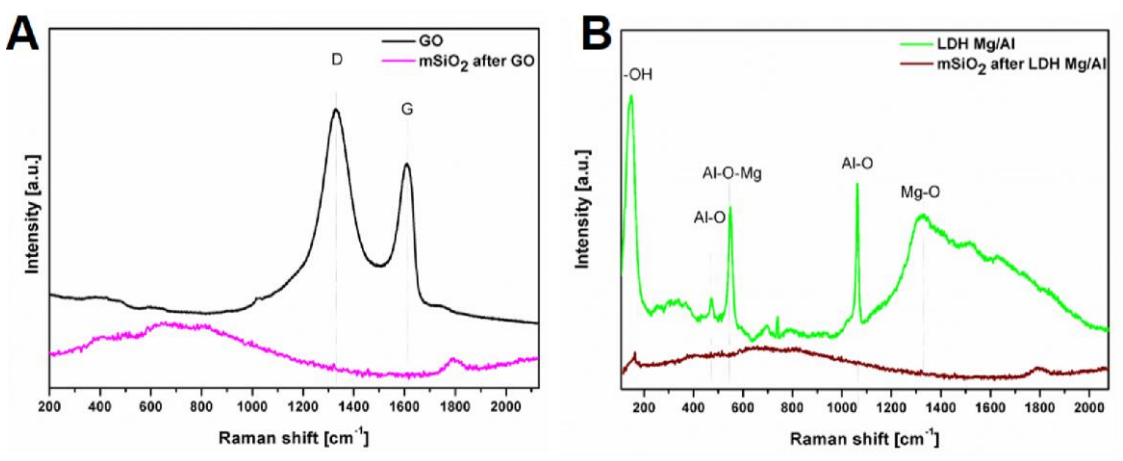

Figure S3. Raman spectra of $mSiO_2$ after GO (**A**) and GO and $mSiO_2$ after LDH Mg/Al and LDH Mg/Al (**B**).

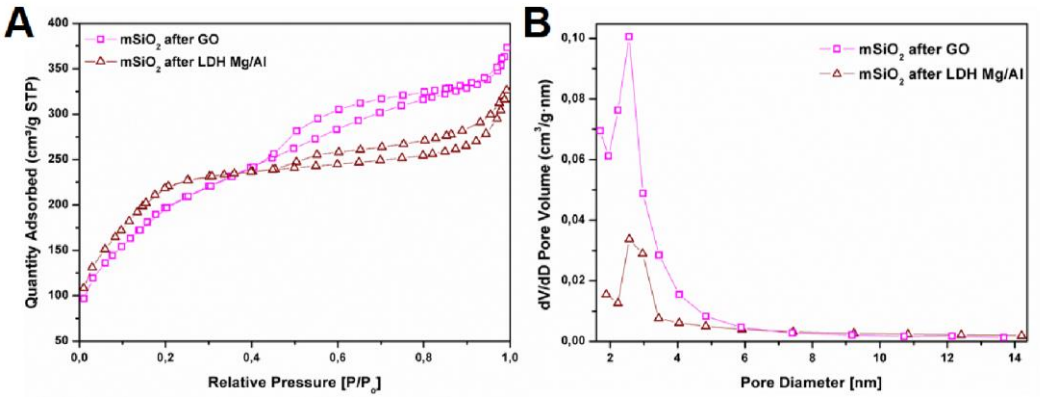

Figure S4. BET isotherms (**A**) and diagrams of pore diameter distribution (**B**) of $mSiO_2$ after GO and $mSiO_2$ after LDH Mg/Al**.**

The thermogravimetric analysis (TGA) of silica flakes functionalized with folic acid is presented in Figure S5. In both samples, there is a weight loss assigned to the removal of moisture (up to 100 °C). Folic acid undergoes combustion in the range between 100 and 600 °C. It was calculated that the sample based on LDH Mg/Al loaded 20 wt % of folic acid, while the silica formed on GO contained 23 wt % of folic acid.

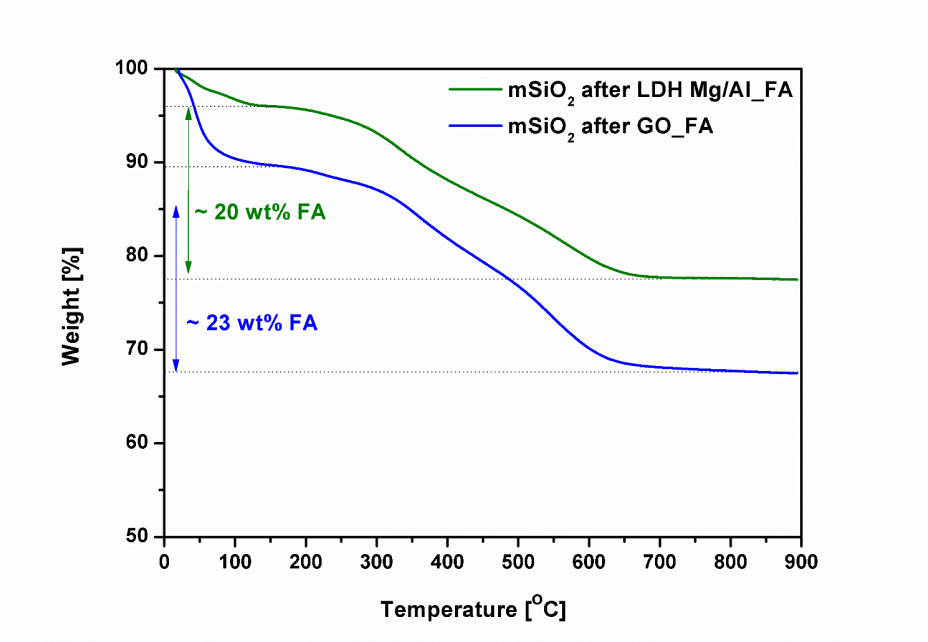

Figure S5. Thermogravimetric analysis of silica flakes functionalized with folic acid**.**

References

1. Roy, I.; Rana, D.; Sarkar, G.; Bhattacharyya, A.; Saha, NR.; Mondal, S.; Pattanayak, S.; Chattopadhyay, S.; Chattopadhyay, D Physical and electrochemical characterization of reduced graphene oxide/silver nanocomposites synthesized by adopting a green approach. *RSC Advances* **2015**, *5*, 25357–25364.
2. Rezaei, B.; Heidarbeigy, M.; Ensafi, AA.; Dinari, M.; Electrochemical Determination of Papaverine on Mg-Al Layered Double Hydroxide/ Graphene Oxide and CNT Modified Carbon Paste Electrode. *IEEE Sens. J.* **2016**, *16*, 3496–3503.
3. Huo, C.; Ouyang, J.; Yang, H.; CuO nanoparticles encapsulated inside Al-MCM-41 mesoporous materials via direct synthetic route. *Sci. Rep.* **2015**, *4*, 3682–3690.
4. Johra, FT.; Lee, J-W.; Jung, WG.; Facile and safe graphene preparation on solution based platform. *J. Ind. Eng. Chem.* **2014**, *20*, 2883–2887.

5. Kingam, KJ.; Hemley, RJ.; Raman spectroscopic study of microcrystalline silica. *Am. Miner.* **1994**, *79*, 269–273.
6. Mrózeka, O.; Ecorchard, P.; Vomáčka, P.; Ederer, J.; Smržová, D.; Šrámová Slušná, M.; Machálková, A.; Nevoralová, M.; Beneš, H Mg-Al-La LDH-MnFe2O4 hybrid material for facile removal of anionic dyes from aqueous solutions. *Appl. Clay Sci.* **2019**, *169*, 1–9.
7. Islam, MR.; Guo, Z.; Rutman, D.; Benson, TJ.; Immobilization of triazabicyclodecene in surfactant modified Mg/Al layered double hydroxides. *RSC Adv.* **2013**, *3*, 24247.
8. Burrueco, MI.; Mora, M.; Jiménez-Sanchidrián, C.; Ruiz, JR.; Raman microspectroscopy of hydrotalcite-like compounds modified with sulphate and sulphonate organic anions. *J. Mol. Struct.* **2013**, *1034*, 38–42.
9. Sieber, T.; Ducke, J.; Rietig, A.; Langner, T.; Acker, J; Recovery of Li(Ni0.33Mn0.33Co0.33)O2 from Lithium-Ion Battery Cathodes: Aspects of Degradation. *Nanomat.* **2019**, *9*, 246–260.
10. Akram, MW.; Fakhar-e-Alam, M.; Butt, AR.; Munir, T.; Ali, A.; Alimgeer, KS.; Mehmood-ur-Rehman, K.; Iqbal, S.; Ali, S.; Ikram, M.; Amin, N.; Wang, ZM.; Magnesium Oxide in Nanodimension: Model for MRI and Multimodal Therapy. *J. Nanomater.* ***2018***, 1–12.